Asian Journal of Chemistry; Vol. 29, No. 4 (2017), 875-878

ASIAN JOURNAL OF CHEMISTRY

https://doi.org/10.14233/ajchem.2017.20340

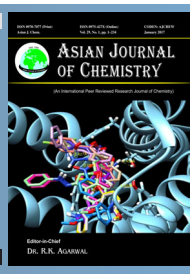

Synthesis of Nano-Crystalline Tin Dioxide and its Effect on Calcination

BENNY SEBASTIAN[1,2,*], C. GEORGE THOMAS[3] and B. MANOJ[3]

[1]Department of Physics, Bharathiar University, Coimbatore-641 046, India
[2]Department of Electronics, Christ University, Bengaluru-560 029, India
[3]Department of Physics, Christ University, Bengaluru-560 029, India

*Corresponding author: E-mail: benny.sebastain@christuniversity.in

Received: 11 October 2016; *Accepted*: 27 December 2016; *Published online*: 31 January 2017; AJC-18263

Nitrate-citrate gel-combustion method was used in this study to prepare nano-crystalline tin dioxide. The samples were calcined at a temperature range of 543-1173 K. The prepared powder was characterized by SEM, TEM and X-ray diffraction. On increasing the temperature with limited supply of air (calcination), there is a systematic increase in tin content accompanied by a reduction in oxygen. The tetragonal nano tin structure formed during the process has about 20 nm in lateral size. With increase in calcination temperature, the carbon content systematically decreased.

Keywords: Nano crystals, Gel-combustion, Calcination.

INTRODUCTION

In recent years inorganic nano-materials have become an active area of research due to their captivating property which are unique from that of their bulk states [1,2]. They have unique physical, chemical and opto-electronic properties owing to their finite size and high surface-to-volume ratio [3,4]. Since the surface to volume ratio is much larger than that commonly found for semiconductor materials both the surface properties and grain boundary distribution become predominant. This renders these materials as good candidates for applications that will take advantage of the high surface to volume ratio, such as chemical sensors or luminescent semiconducting sensors [5]. They have numerous applications such as photo catalysts, battery materials, solid state gas sensor devices and optoelectronic devices. This is due to their quantum confinement effect and size and shape-dependent characteristics [2]. Oxides exhibit an extensive range of electrical properties which vary from wide band-gap insulators to metallic and superconducting. This makes them a potential candidate for industrial applications.

Owing to their electrical properties and potential applications in the field of material science, SnO_2 nanostructures have been identified as one of the most essential oxide nanostructures. It is an important n-type wide band gap (E_g = 3.64 eV at 300 K) semiconductor [1,6]. The key for understanding many aspects of SnO_2, surface properties is the dual valency of Sn. Tin dioxide belongs to a class of materials that combines high electrical conductivity with optical transparency in the visible range of electromagnetic spectrum.They also reflect infrared light and exhibit good chemical and mechanical stability [7,8]. The most important use of SnO_2 is that of an active layer in gas-sensing devices, for the detection of noxious and explosive gases such as hydrogen, carbon monoxide, ethanol and methanol [4,5,7-9]. They exhibit changes in electrical resistivity in the presence of certain gases [4]. The sensing properties of SnO_2 sensors such as reproducibility sensitivity and selectivity greatly dependent on several factors, which include size and particle distribution as well as specific surface area. These morphological traits contribute great significance due to the fact that surface reactions are more relevant than bulk changes. During the reactions between surface oxygen species and reducing gases like CO and alcohol are to be detected. This can be enhanced by increasing the sensing surface area [10]. The sensitivity is set to increase sharply as crystalline size decreases below a critical value [11].

Due to these properties of SnO_2, there is a great industrial and commercial demands for reproducible low cost synthesis methods. Tin dioxide nanoparticles are prepared by various methods such as sol-gel, hydrothermal, co-precipitation, spray pyrolysis, electrochemical deposition laser ablation and micro emulsions technique [3]. Out of these different techniques, co-precipitation is less expensive and easy to implement especially when it is compared with sol-gel method. But, the chloride ions could also contaminate the material and thereby changing the surface and electrical properties. In this current

work facile synthesis of SnO_2 nanoparticles by a novel gel combustion technique is reported. The effect of calcination on the lateral size of the nano tin crystals is also highlighted.

EXPERIMENTAL

Synthesis of SnO_2 nano crystalline: Tin oxide nanoparticles were prepared by nitrate-citrate gel combustion technique which was followed by calcination at high temperatures. Nitric acid was used to provide the oxidizing ions while the fuel used was citric acid which is also the reducing agent. Metallic tin of purity 99.9 % was used for the production of SnO_2 nanoparticles. An aqueous solution of pure metallic tin (1 g) dissolved in nitric acid (50 mL) along with citric acid (50 mL) and ammonium hydroxide (50 mL). The solution was heated in a magnetic stirrer at 363 K in a borosil vessel without producing any precipitation. The solution was heated till it turned into a white viscous gel.

The resultant gel was heated on a hot plate under high temperature. When the temperature is above 543 K the gel then undergoes a strong self propagating combustion reaction which is highly exothermic due to the reaction between nitrate and citrate ions. This leads to emission of large amountof non-toxic gases. This process promotes the disintegration of the precursor thereby producing nano-crystalline particles. The entire process was over within 3-4 min. Citric acid not only works as the fuel for the exothermic reactions but also it forms tin complexes which prevents hydroxylated tin compounds. The synthesized materials were collected and calcined at different temperatures (543, 673, 773, 873, 1023 and 1173 K) for about 1 h for the decomposition of the carbonaceous residues. The samples were characterized by XRD, SEM and TEM.

The whole process is summarized as follows:

$$2HNO_3 \longrightarrow H_2O + 2NO_2 + O \quad (1)$$

$$Sn + O \longrightarrow SnO \quad (2)$$

$$2HNO_3 + Sn \longrightarrow H_2O + 2NO_2 + SnO \quad (3)$$

$$SnO + 2HNO_3 \longrightarrow Sn(NO_3)_2 + H_2O \quad (4)$$

$$Sn(NO_3)_2 + NH_4OH \longrightarrow Sn(OH_2) + 2NH_4NO_3 \quad (5)$$

$$3Sn(OH_2) + 2C_6H_8O_7 \longrightarrow (C_{12}H_{10}O_{14})Sn_3 + 6H_2O \quad (6)$$

$$(C_{12}H_{10}O_{14})Sn_3 + O_2 \longrightarrow SnO_2 + 2CO_2 + 5H_2O \quad (7)$$

Characterization: The phase identification and size of the nanocrystalline tin dioxide were obtained by X-ray powder diffraction (XRD) using (Bruker AXS D8 advance) with CuK_α radiation (λ = 1.5418 Å). Data were collected in the 2θ range from 20° to 60°. In order to calculate the crystallite size, the Scherrer formula was used:

$$D = 0.94\ \lambda/\beta \cos\theta \text{ [12,13]} \quad (8)$$

where D is the average size of the crystal, λ is the wavelength, β is the corrected line width at half-peak intensity and θ is the diffraction peak angle. Scanning electron microscopy (SEM, Joel model JSM-6390 LV) and TEM (Jeol/JEM 2100) techniques are used in order to study the surface morphology.

RESULTS AND DISCUSSION

Structural characterization: The synthesized nano crystalline tin dioxide is calcined at different temperatures to the structural modification. The X-ray analysis of the product obtained is depicted in Fig. 1.

X-ray diffraction pattern shows peaks at 2θ values of 26.60°, 33.80°, 37.90°, 51.80° of tin dioxide nanoparticles (Fig. 1). These values can be associated with (110), (101), (200), (211), (220) plane of the tin oxide. The sharp diffraction peak at respective diffraction angles also indicate high degree of crystallization with calcination. As the temperature increases the peak at 33.8 shift to lower angle and a broadened profile is formed at 1173 K. The 51.80° peak also shows a similar trend but disappeared at 1173 K. The X-ray diffraction profile shows rapid changes with calcination. It was also observed a broadened amorphous peak owing to the content of carbon in the samples.

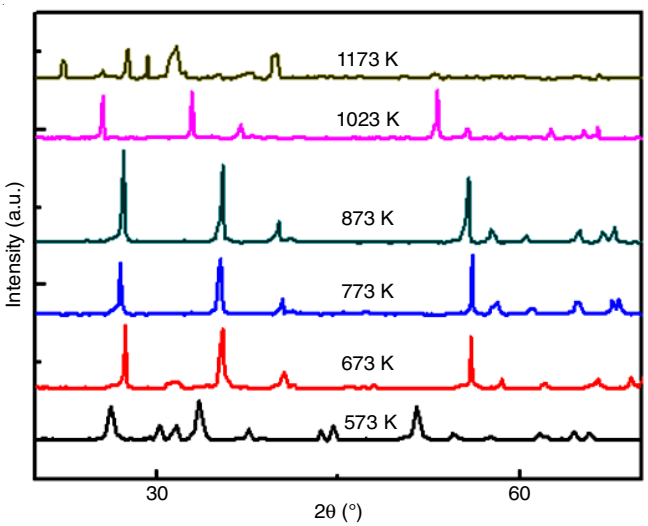

Fig. 1. XRD pattern of the SnO_2 nanoparticle at various temperatures

In the 2θ about 34° region, the non-symmetrical line shape originated from the broadening of the peak 101 (Fig. 1). The structural parameters of the synthesized nanostructure is elucidated with modified Scherrer formula [12-19] and is presented in Table-1.

TABLE-1
D VALUES FROM XRD PATTERN
USING SCHERRER FORMULA

Temperature of calcinations (K)	D (nm) Lateral dimension
543	19.23
673	17.86
773	16.13
873	19.92
1023	23.90
1173	23.93

We found the FWHM of the peak obtained at 34.3° and the particle size was found to be in the range of 16-24 nm. The size of the particle initially decreased with the increasing calcination temperature. At high temperature, it is again increased and become constant at 23.9 nm and optimized.

Morphological characterization: Fig. 2 shows the SEM images of the resulted SnO_2 nano structures by combustion and calcination process. In order to remove the carbon content present in the samples and to make the sample more suitable for the application purposes, the SnO_2 powder obtained calcined at different temperatures as shown in Fig. 2 (a-543 K), (b-773 K) and (c-1023 K) and (d-1173 K). At lower temperature the nanostructure was evident as particle and at high temperature the silky layers are formed. The surface looks more uniform. Flakes are also noticed. It is an indication of crystalline structure is formed.

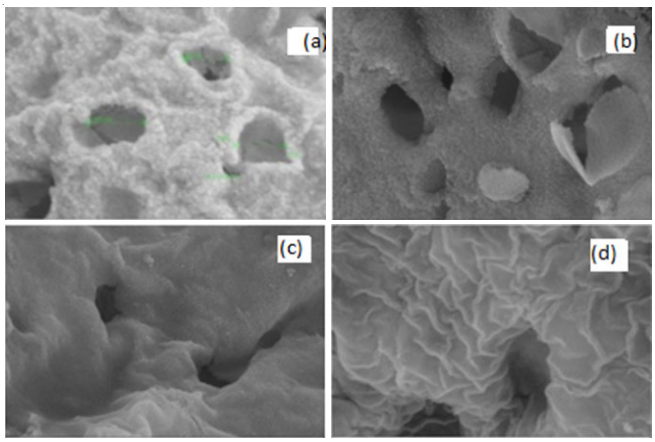

Fig. 2. SEM images of SnO_2 nanoparticles at different temperatures

As the temperature increases to 1023 K, the particle size decreases and the surface looks like a silky form as shown in Fig. 2(d).

TEM analysis of the product was carried out and is presented in Fig. 3. It revealed that most of the nanoparticles are highly agglomerated and nearly spherical shape with size around 20 nm. The crystalline size observed by TEM is in good agreement with that calculated using Scherrer formula from XRD analysis as shown in Table-1. The SAED pattern as shown in Fig. 3(b) exhibits continuous ring pattern indicating the nanosized and highly crystalline nature of the SnO_2 particles. Multiple rings are seen in SAED spectrum, as expected from the XRD pattern. The bright field image confirms that the nanoparticle are spherical in shape and have a narrow distribution of the particle size [4]. The Fig. 3(d) reveals the crystalline nature of the sample higher at high temperature. Fig. 3(e&f) shows the lattice fringes, which is about 0.33 nm attributed to the (110) plane of the rutile structure of nano crystalline tin oxide. The TEM images are supporting the findings of the X-ray and FE-SEM analysis [13,20].

Conclusion

Synthesis of nano crystalline SnO_2 by auto ignition of a citrate-nitrate gel method has been reported. Pure and single crystalline SnO_2 was successfully synthesized *via* sol-gel combustion process using tin nitrate as precursor. During the study, it was observed that when the gel was heated, a highly exothermic reaction between nitrate and citrate ions took place. The temperature required for the phase transformation was given by the reaction itself. The diffraction peaks observed in the XRD pattern indicates crystallization in the SnO_2 nanoparticles. The size of the particles prepared was of nanometric range and calculated using Scherer's formula from the XRD pattern and it was found to be 16 to 23 nm. SEM and TEM images reveal the formation of crystalline SnO_2 nanoparticles. SAED pattern showed continuous ring pattern which indicates nano crystalline nature. Some of the important applications of SnO_2 areas catalysts, energy-saving coatings, preparation of liquid crystal displays, gas sensors, optoelectronic devices are worth investigating.It is a low temperature process in which

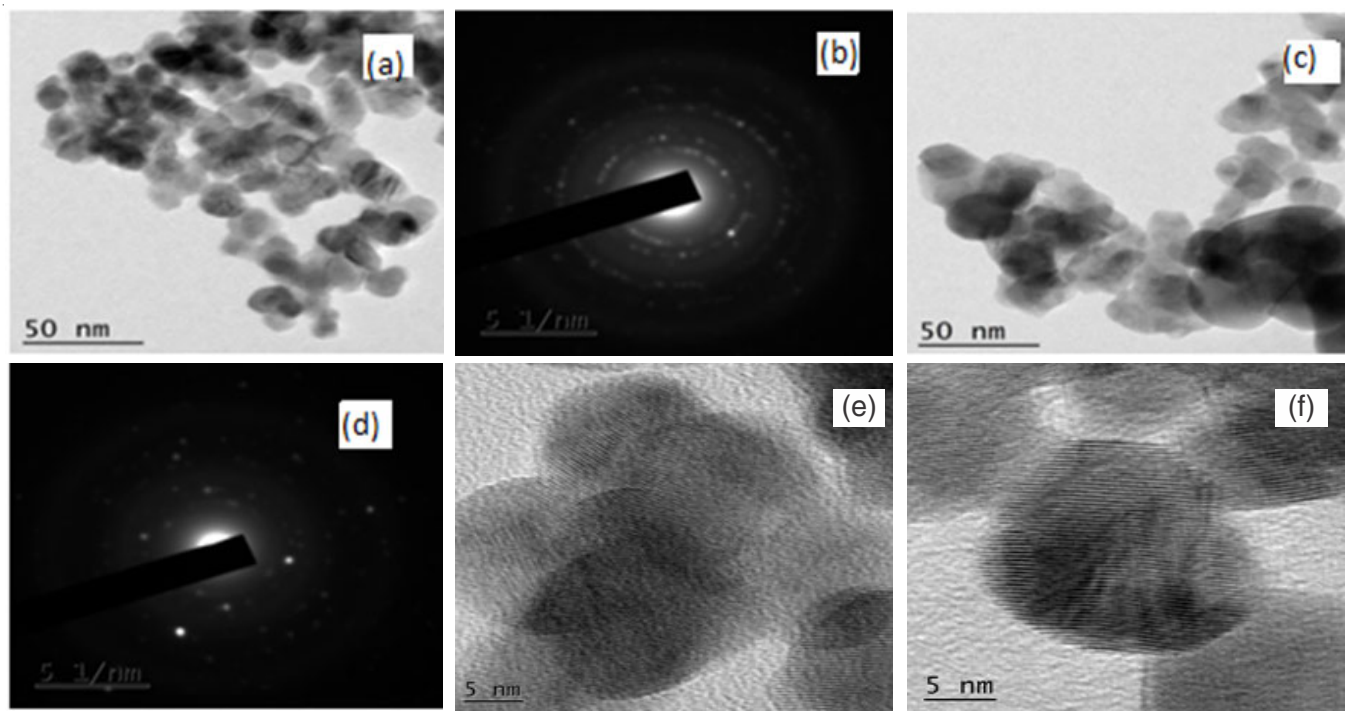

Fig. 3. TEM images ofSnO_2 nanoparticles at different temperatures

final products are formed almost instantaneously due to the exothermic reaction.

REFERENCES

1. S. Raghuwanshi, V. Kumar and R. Pandey, *Int. Nano Lett.*, **2**, 2 (2012); https://doi.org/10.1186/2228-5326-2-2.
2. H. Elhamzaoui, B. Jousseaume, T. Toupancea and C. Zakrib, *Dalton Trans.*, **23**, 4429 (2009); https://doi.org/10.1039/B901757G.
3. V.S. Kundu, R.L. Dhiman, D. Singh and A.S. Maan, *Int. J. Adv. Res. Sci. Eng.*, **2**, 15 (2013).
4. A. Ayeshamariam, C. Sanjeeviraja and and R.P. Samy, *J. Photonics Spintronics*, **2**, 4 (2013).
5. C. Nayral, E. Viala, P. Fau, F. Senocq, J.-C. Jumas, A. Maisonnat and B. Chaudret, *Chem. Eur. J.*, **6**, 4082 (2000); https://doi.org/10.1002/1521-3765(20001117)6:22<4082::AID-CHEM4082>3.0.CO;2-S.
6. S. Blessi, M.M. Lumina Sonia, S. Vijayalakshmi and S. Pauline, *Int. J. Chem. Tech. Res.*, **6**, 2153 (2014).
7. M. Batzill and U. Diebold, *Prog. Surf. Sci.*, **79**, 47 (2005); https://doi.org/10.1016/j.progsurf.2005.09.002.
8. S. de Monredon, A. Cellot, F. Ribot, C. Sanchez, L. Armelao, L. Gueneau and L. Delattre, *J. Mater. Chem.*, **12**, 2396 (2002); https://doi.org/10.1039/b203049g.
9. L.B. Fraigi, D.G. Lamas and N.E. Walsöe de Reca, *Mater. Lett.*, **47**, 262 (2001); https://doi.org/10.1016/S0167-577X(00)00246-9.
10. L. Fraigi, D.G. Lamas and N.E. Walsöe de Reca, *Nanostruct. Mater.*, **11**, 311 (1999); https://doi.org/10.1016/S0965-9773(99)00046-X.
11. M.A. Farrukh, *Turk. J. Chem.*, **34**, 537 (2010).
12. Chaoumead, W.-J. Choi, D.-H. Lee and Y.-M. Sung, *J. Electr. Eng. Technol.*, **6**, 414 (2011); https://doi.org/10.5370/JEET.2011.6.3.414.
13. A.N. Naje, A.S. Norry and A.M. Suhail, *Int. J. Innov. Res. Sci., Eng. Technol.*, **2**, 7068 (2013).
14. B. Manoj, *Int. J. Min. Met. Mater.*, **21**, 940 (2014); https://doi.org/10.1007/s12613-014-0993-7.
15. J. Gajendran and V. Rajendran, *Int. J. Mater. Biomater. Appl.*, **2**, 37 (2012).
16. X.M. Liu, S.L. Wu, P.K. Chu, J. Zheng and S.L. Li, *Mater. Sci. Eng. A*, **426**, 274 (2006); https://doi.org/10.1016/j.msea.2006.04.032.
17. B. Manoj, *Asian J. Chem.*, **26**, 4553 (2014); https://doi.org/10.14233/ajchem.2014.15150.
18. B. Manoj, *Russian J. Phys. Chem. A*, **89**, 2438 (2015); https://doi.org/10.1134/S0036024415130257.
19. A.V. Ramya, A. Mohan and B. Manoj, *Mater. Sci.-Poland*, **34**, 330 (2016); https://doi.org/10.1515/msp-2016-0061.
20. K. Anandan and V. Rajendran, *J. Non-oxide Glasses*, **2**, 83 (2010).